Predicting the wet collapse pressure for flexible risers with initial ovalization and gap An analytical solution

Li, Xiao; Jiang, Xiaoli; Hopman, Hans

DOI
10.1016/j.marstruc.2020.102732

Publication date
2020

Document Version
Final published version

Published in
Marine Structures

Marine Structures 71 (2020) 102732

Contents lists available at ScienceDirect

Marine Structures

journal homepage: http://www.elsevier.com/locate/marstruc

Predicting the wet collapse pressure for flexible risers with initial ovalization and gap: An analytical solution

Xiao Li *, Xiaoli Jiang, Hans Hopman

Department of Maritime and Transport Technology, Delft University of Technology, Netherlands

ARTICLE INFO

Keywords:
Flexible pipes
Critical pressure
Ovalization
Radial gap
Wet collapse

ABSTRACT

As offshore hydrocarbon production moves towards ultra-deep water, flexible risers have to withstand the huge hydro-static pressure without collapse. They are designed with strong collapse capacities, allowing them to operate under the condition where their annuli are flooded by the seawater. However, initial imperfections can weaken the collapse capacity under such a flooded condition, triggering the so-called "wet collapse". Two common initial imperfections, the carcass ovality and the radial gap between the carcass and pressure armor, would reduce the collapse strength of flexible risers significantly. Mostly, collapse analyses are performed through numerical simulations, which are less feasible for the design stage of flexible risers comparing with analytical models. To date, there are few analytical models available in public literature to predict the wet collapse pressure of flexible risers accounting for initial ovality and gap. To meet this demand, an analytical model is established in this paper to address these issues. This model is developed as a spring-supported arch, solving the collapse pressure with stability theories of ring and arched structures. This analytical model is verified by numerical simulations, which gives prediction results that correlate well with the numerical ones.

1. Introduction

Flexible risers are multi-layer pipe structures which offer the operators a robust method to exploit hydrocarbon products in harsh ocean environments [1]. A typical flexible riser is designed using a mixture of helical wound armor wires and polymeric sheaths, which enables this structure a unique flexibility to withstand large dynamic motions imposed by floating units [2]. Fig. 1 illustrates the main layers in a flexible pipe [3]. The carcass and pressure amour are two self-interlocking layers which provide resistances to external and internal pressure, separately. The polymeric inner layer in-between acts as a water barrier which contains fluids within the pipe bore. Tensile armor usually forms in pairs to take the tension, bending and twist loads. The outer sheath is the outermost polymeric layer to help prevent the riser annulus from being flooded by seawater.

As the oil and gas production is heading towards the ultra-deep water reservoirs at a depth of 3000 m or more, higher collapse resistance of flexible risers is being required to counter the huge hydro-static pressure [4–6]. Normally, the external pressure is resisted by all the layers within the riser body. However, the frequent movements of flexible risers on the seabed can damage the outer sheath [7], leading to a flooded annulus. In this situation, the carcass and pressure armor are the main layers for collapse resistance, as they contribute the most to the riser radial stiffness. Once the external pressure exceeds the collapse capacity of a flexible riser, the collapse failure occurs, which is referred as "wet collapse" [8].

* Corresponding author.
E-mail address: X.Li-9@tudelft.nl (X. Li).

https://doi.org/10.1016/j.marstruc.2020.102732
Received 1 May 2019; Received in revised form 7 January 2020; Accepted 30 January 2020
Available online 10 February 2020

Mostly, the wet collapse pressure is higher than the collapse limit of the carcass because of the radial constraints provided by the surrounded pressure armor [9]. However, this critical pressure might be reduced by two initial imperfections: ovalization of the carcass, and inter-layer gap between the carcass/liner and pressure armor. The ovalization of the carcass is a defect generated from the manufacture process while the inter-layer gap is caused by the volume change or extrusion of the liner [10,11], as shown in Fig. 2 [12]. Although tensile armors can reduce the interlayer gaps by squeezing the pressure armor, it is hard to close these gaps completely if the pipe is under a low longitudinal tension. For a flexible riser facing the flooded annulus situation, its collapse strength is sensitive to those two imperfections [10,11,13,14]. Besides, those imperfections may also affect the collapse modes of an encased carcass [15]. Collapse is known to take place as two modes, one is called "heart" (singly symmetric) mode and the other is "eight" (doubly symmetric) mode [16,17], as shown in Fig. 3. Critical pressure of the confined carcass corresponds to each collapse mode would be different.

To date, most collapse analyses of flexible pipes on initial imperfections were conducted numerically. This is less feasible for the design stage of flexible risers. Although analytical approaches are usually a first natural choice for predicting the collapse pressure of flexible risers, there are few of them available in public literature to address the initial imperfections [18]. To meet this demand, an analytical model is presented in this paper. This analytical model is developed based on the stability theories of ring and arched structures, which could take the initial ovality and inter-layer gap into account. Additionally, this model is able to consider either "heart" or "eight" collapse mode based on the imposed initial ovalization type. The content of this paper is organized as follows: Section 2 summarizes the analytical models that have been developed for predicting the critical pressure and their limitations for addressing the initial geometric imperfections of flexible pipes. After that, an analytical approach for assessing the collapse strength of the flexible pipes with initial imperfections is presented in Section 3. In Section 4, numerical simulation is employed to check the reliability of the proposed analytical approach with case studies. Conclusions are drawn in the final section.

We note that a shorter conference version [19] of this paper appeared in OMAE 2019 conference. Our initial conference paper did not address the problem of collapse modes. This issue is addressed in this paper and corresponding analyses along with the case studies are also presented.

2. Existing analytical models for collapse prediction

Although collapse of flexible risers has been studied for years, the analytical models, for the most part, are developed from ring buckling theories [20].

$$P_{\mathrm{cr}} = \frac{3EI}{(1-\upsilon^2)R^3} \tag{1}$$

where E and υ are respectively the Young's Modulus and Poisson's ratio of the material; I is the inertia moment and R is the ring radius; P_{cr} is the elastic critical pressure.

If no radial gaps are present between the layers, the sum of elastic collapse pressure from the carcass and pressure armor is regarded as the critical pressure of the whole flexible pipes [21].

$$P_{\mathrm{cr}} = \sum_{n=1}^{N_p} \frac{3(EI)_n}{(1-\upsilon^2)R_n^3} \tag{2}$$

where the subscript 'n' represents the parameters of corresponding metallic layers, N_p denotes the number of the related layers. However, such a formula is not applicable for the wet collapse situation. The wet collapse of flexible pipes can be described as the radial buckling of the confined carcass under external pressure [9]. In terms of this kind of buckling, a closed-form analytical solution of a thin-walled ring confined in a rigid cavity was presented by Glock [22].

$$P_{\mathrm{cr}} = \frac{EI}{1-\upsilon^2}\left(\frac{t}{D}\right)^{2.2} \tag{3}$$

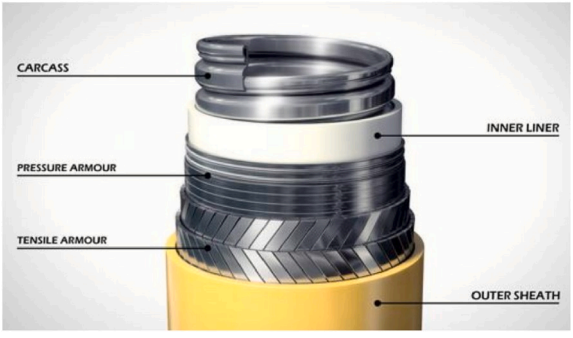

Fig. 1. Typical configuration of a flexible riser [3].

Fig. 2. Extrusion of the liner into the adjacent interlocked carcass [12].

Fig. 3. "Heart" mode (left) [16] and "Eight" mode (right) [17].

where t is thickness of the cylinder and D is the mean diameter. Glock's formula was then extended [23,24] to consider a tightly (small gap) or loosely fitted (large gap) concentric rings. Although those formulae could consider the gap effect, they overestimate the critical pressure of flexible pipes since the pressure armor supports the carcass more like an elastic medium rather than a rigid cavity. In this regard, an elastic ring model with horizontal spring supports was proposed in Ref. [9]. This model treats the pressure armor as springs which support the inner carcass at the horizontal direction, as depicted in Fig. 4.

With this model, the formula for predicting the collapse pressure of the carcass takes the form

$$P_{cr} = \frac{3E_i I_i}{R_i^3} + \frac{2}{3}\frac{8E_o I_o}{(\pi^2 - 7)R_o^3} \tag{4}$$

where the subscripts 'i' and 'o' represent the inner and outer ring, separately. This model gives an elastic solution of the critical pressure for the risers subjected to wet collapse, without considering the effects of initial imperfections. For the flexible risers used in deep water condition, however, collapse usually occurs with the material plasticity of the inner carcass layers [25], especially under the influences of initial imperfections.

Although various models have been proposed as listed above, a well-developed analytical model is still lacking for initial imperfection issues of the flexible riser with a plastic wet collapse. To meet this demand, an analytical model is established in the following

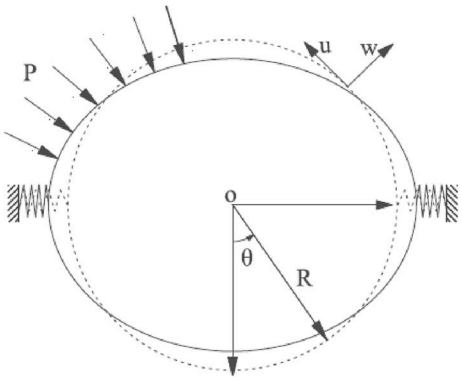

Fig. 4. Buckling of the inner cylinder with spring supports [9].

section based on the stability theories of ring and arched structures.

3. Analytical model for initial imperfections

For conventional steel pipes, their plastic collapse pressure can be determined based on the assumption given by Timoshenko and Gere [20], which has a definition as: pipe collapses when its maximum hoop compressive stress reaches the material yield stress. This assumption is also adopted in our model development for the wet collapse of flexible risers. The wet collapse pressure can be solved by equaling the maximum hoop compressive stress of the carcass (or its equivalent layer) to its material yield stress.

Such a wet collapse pressure is not easy to be determined for flexible pipes, especially for the ones with initial imperfections. For a carcass confined by the pressure armor, it would go through two different collapse phases if there is an interlayer gap in-between. Depending on whether the gap closes or not, the whole collapse process can be divided as: pre-contact and post-contact phases, as depicted in Fig. 5. During the pre-contact phase, the carcass and inner liner are deformed together as a buckled single layer ring. The pressure armor provides no constraints on the radial deformation of the carcass/liner in this period. Once the contact occurs, the carcass starts to be divided into two portions: attached and detached portions. During this post-contact phase, the wet collapse pressure of the carcass is dominated by the buckling strength of the detached portion.

The presented analytical approach adopts two sub-models for each phase. For the pre-contact phase, formulae of the ring buckling are used to solve the external pressure P_{con} that making the contact occurs. For the post-contact phase, formulae of the arch buckling are employed to determine the plastic buckling pressure P_{arch} of the detached portion. With those two sub-models, the wet collapse pressure of a flexible riser with initial imperfections is the sum of P_{con} and P_{arch}.

3.1. Pre-contact phase

For a flexible pipe with all layers are perfectly circular, the initial gap is the radial gap span between the liner and the pressure armor. If the carcass together with the liner is in an ovalized shape initially, then the initial gap is minimum radial gap span ω_g between the layers, as shown in Fig. 6. The carcass encased in the pressure armor may experience two different buckling situations, depending on the value of the interlayer gap. If the gap width is large enough, the inner carcass collapses as a single ring; otherwise, layer contact occurs, followed by the post-contact phase.

Due to the initial ovality from the manufacturing process, the carcass always deviates from a perfect circularity (the dash line) with a small deflection ω_0. This initial deflection can be calculated according to the definition of ovalization given in API 17B (2014) [26]. For the above-mentioned first situation, the plastic collapse of such an ovalized carcass can be calculated with the formula given as follow [20].

$$P_y^2 - \left[\frac{\sigma_y t_c}{R_c} + \left(1 + 6\frac{\omega_0}{t_c}P_{cr}\right)\right]P_y + \frac{\sigma_y t_c}{R_c}P_{cr} = 0 \tag{5}$$

where ω_0 is the initial radial deflection of the carcass, depending on its initial ovality; σ_y is the material yielding stress; R_c and t_c are mean radius and equivalent thickness of the carcass; P_{cr} is the elastic critical pressure obtained from Eq. (1); P_y is the plastic critical pressure of the single carcass layer. And the maximum horizontal displacement ω_{max} of the point H on the carcass under that plastic collapse pressure can be obtained by Ref. [20].

$$\omega_{max} = \frac{\omega_0 P_y}{P_{cr} - P_y} \tag{6}$$

where ω_{max} is the maximum radial deformation of the carcass. If the gap width ω_g is smaller than ω_{max}, then the radial deformation of the inner carcass is restrained after the closure of gaps. In this situation, the external pressure at the contact moment can be determined by the gap width ω_g, which is given as

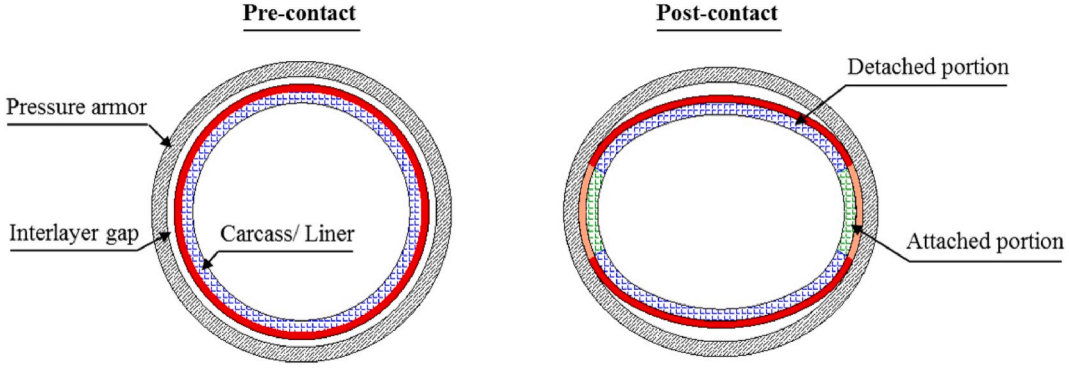

Fig. 5. Progressive buckling process of an encased carcass in wet collapse.

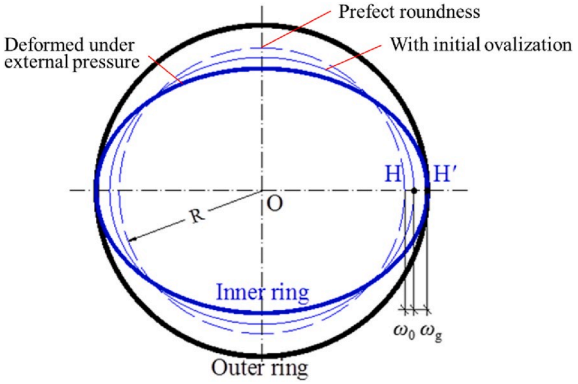

Fig. 6. Contact moment of a concentric ring structure.

$$P_{con} = \frac{\omega_g P_{cr}}{\omega_g + \omega_0} \tag{7}$$

where P_{con} is the external pressure at the moment in which the carcass start to contact the pressure armor. However, it should be noted that the external pressure could cause a reduction on the wall thickness of the inner liner due to its elastic deformation. This reduction postpones that contact moment between the carcass/liner and pressure armor. Thus, Eq. (7) should be improved as

$$\begin{cases} P_{con} = \dfrac{(\omega_g + t_{lr})P_{cr}}{\omega_g + \omega_0 + t_{lr}} \\ t_{lr} = t_{lr}(P_{con}) \end{cases} \tag{8}$$

where t_{lr} is the reduction of wall thickness of the liner. Both the P_{con} and t_{lr} can be determined by substituting the material constitutive equation of the liner into Eq. (8). Moreover, the maximum hoop compressive stress at the crown point of the carcass under the external pressure P_{con} is

$$\sigma_{con} = \frac{P_{con}R_c}{t_c} + \frac{6P_{con}R_c}{t_c^2}\frac{\omega_0}{1 - P_{con}/P_{cr}} \tag{9}$$

After obtaining this maximum compressive stress, the following task is to work out how much additional external pressure is demanded in the post-contact phase for reaching the material yield stress of the carcass.

3.2. Post-contact phase

Once the carcass/liner contact the surrounded pressure armor, the attached portion starts to extends in the hoop direction until the critical pressure is reached [27], as shown in Fig. 7. The initial ovalization and interlayer gap guide the carcass to deform in either

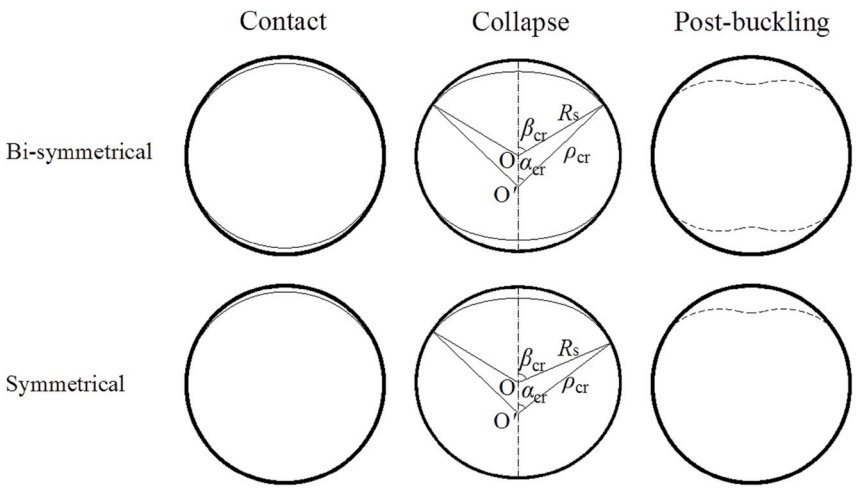

Fig. 7. Progressive buckling process during the post-contact phase.

symmetrical or bi-symmetrical shape, leading to the "heart" or "eight" mode.

The detached portion can be regarded as a circular arch with a new center O'. The geometry of this arch is determined by initial imperfections together with the collapse shapes. When the point where the carcass/liner separates from the pressure armor at the moment of collapse is determined, the geometry of this circular arch can be calculated for the carcass in either bi-symmetrical or symmetrical shapes:

$$\text{Bi}-\text{symmetrical} \quad \begin{cases} 2\pi R_c - 2R_s(\pi - 2\beta) = 4\alpha\rho \\ \rho\sin\alpha = R_s\sin\beta \end{cases} \tag{10}$$

$$\text{Symmetrical} \quad \begin{cases} 2\pi R_c - 2R_s(\pi - \beta) = 2\alpha\rho \\ \rho\sin\alpha = R_s\sin\beta \end{cases} \tag{11}$$

where R_s is the distance from the separation point to the ring center at the collapse moment; ρ is the arch radius referred to the new center O'; α and β are the angular quantities displayed in Fig. 7; subscript 'cr' represents the parameters at the moment of collapse.

Although this arch is detached from the surrounded pressure armor, the radial deformation of the arch ends is still restrained. Since the pressure armor confines the carcass as an elastic medium, it is treated as springs that support at the arch ends. Therefore, a spring-supported arch model is proposed for this collapse issue, as shown in Fig. 8. The general linear equilibrium equation set for the differential element of a circular arch is expressed as [28].

$$\begin{cases} Q_x^{'} - N + q_x\rho = 0 \\ N^{'} + Q_x + q_z\rho = 0 \\ M^{'} + Q_x\rho = 0 \end{cases} \tag{12}$$

where M, N, and Q_x are the bending moment, hoop force and radial shear force on the differential element; superscript ' represents $\frac{\partial}{\partial\theta}$; θ is the angle for an arbitrary cross section of the arch; q_x and q_z are the uniform loads along the radial and circumferential directions, as shown in Fig. 9. In the wet collapse situation, values of the external loads are given by

$$\begin{cases} q_x = -q = -(P - P_{con}) \\ q_z = 0 \end{cases} \tag{13}$$

where q is the differential pressure between the external pressure P and the pressure P_{con} at the contact moment. Using displacements to reformulate Eq. (12), then

$$\begin{cases} -E_cA_c\dfrac{w'' + u'}{\rho} = 0 \\ E_cA_c\dfrac{w' + u}{\rho} + \dfrac{E_cI_c}{\rho^3}\left(u^{IV} + 2u'' + u\right) = -\rho q \end{cases} \tag{14}$$

where u and w are displacements of the differential element along the radial and circumferential directions, separately; A denotes the cross-sectional area; the items with subscript 'c' refer to the parameters of the carcass. If taking K as

$$K = -\frac{\rho^3}{E_cI_c}\left(\rho q + E_cA_c\frac{w' + u}{\rho}\right) \tag{15}$$

Then the general solution of Eq. (14) can be written as

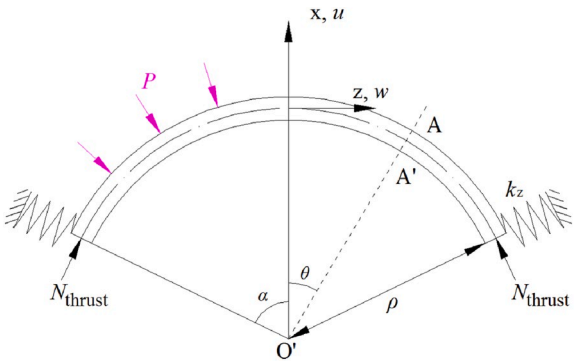

Fig. 8. A spring-supported arch model for the post-contact phase.

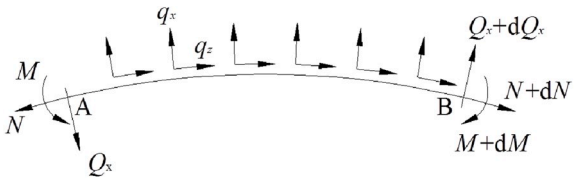

Fig. 9. Equilibrium of a differential element of the arch [28].

$$\begin{cases} u = KC_1\cos\theta + KC_2\theta\sin\theta + K \\ w = -KC_1\sin\theta - KC_2(\sin\theta - \theta\cos\theta) + KC_3\theta \end{cases} \tag{16}$$

where C_1 ~ C_3 are constants that determined by the boundary conditions, and therefore, the forces at any cross section, defined by the angle θ, are

$$\begin{cases} N = \dfrac{E_cA_cK}{\rho}(1 + C_3) + \dfrac{E_cI_cK}{\rho^3}(1 + 2C_2\cos\theta) \\ M = \dfrac{E_cI_cK}{\rho^2}(2C_2\cos\theta + 1) \\ Q_x = \dfrac{E_cI_cK}{\rho^3}(2C_2\sin\theta) \end{cases} \tag{17}$$

For a spring-supported arch model as depicted in Fig. 8, it has boundary conditions at its arch ends as

$$\begin{cases} w|_{\theta=\alpha} = 0, \text{No hoop displacement} \\ N|_{\theta=\alpha} = N_{\text{thrust}}, \text{Force equilibrium in hoop direction} \\ Q_x + k_t u = 0, \text{Force equilibrium in radial direction} \end{cases} \tag{18}$$

where N_{thrust} is the hoop thrust force at the arch end; k_t is the elastic stiffness of the pressure armor together with the liner. The liner between the carcass and pressure armor reduces the support effect of the pressure armor due to its low stiffness. According to Ref. [25], the liner and pressure armor should be considered as two series of springs that supporting the carcass. Therefore, the value of k_t takes form as

$$k_t = \frac{k_p k_l}{k_p + k_l} \tag{19}$$

where k_p and k_l are the elastic stiffness of the pressure and the liner, separately. They can be calculated by referring to the equations in Ref. [25]. The formula for calculating the thrust force N_{thrust} at the arch ends is given as

$$N_{\text{thrust}} = \left[0.65\frac{E_cI_c}{R_c^2}\left(\frac{\pi}{\beta}\right)^2\right]\left(1 - \frac{\omega_g + t_{lr}}{\omega_{\max}}\right)^{\varphi_k^{-0.7}}\left(1 - \frac{\omega_0 + \omega_g + t_{lr}}{R_c}\right) \tag{20}$$

which is improved from the formula given by Glock [22] with non-linear regression analysis. Where φ_k is the bending stiffness ratio of the liner/pressure armor to the inner carcass, which is given as [9].

$$\varphi_k = \frac{k_t}{k_c} \tag{21}$$

with the above boundary conditions, the formulae of C_1 ~ C_3 can be derived

$$\begin{cases} C_1 = \dfrac{D_5}{D_6} - \dfrac{D_4}{D_3D_6}k_t \\ C_2 = (1 + C_1\cos\alpha)\dfrac{k_t}{D_3} \\ C_3 = \dfrac{C_1\sin\alpha + C_2(\sin\alpha - \alpha\cos\alpha)}{\alpha} \end{cases} \tag{22}$$

And the coefficients in Eq. (22) can be calculated as

$$\begin{cases} D_1 = \dfrac{E_c A_c}{\rho}, D_2 = \dfrac{E_c I_c}{\rho^3} \\ D_3 = (2D_2 - k_t\alpha)\sin\alpha, D_4 = D_1\dfrac{\sin\alpha - \alpha\cos\alpha}{\alpha} + 2D_2\cos\alpha \\ D_5 = -\left(\dfrac{N_{thrust}}{K} + D_1 + D_2\right) \\ D_6 = D_1\dfrac{\sin\alpha}{\alpha} + \dfrac{D_4}{D_3}k_t\cos\alpha \\ D_7 = \dfrac{\sin\alpha}{\alpha D_6} + k_t\dfrac{\cos\alpha}{D_3 D_6}\dfrac{\sin\alpha - \alpha\cos\alpha}{\alpha} \\ D_8 = -\dfrac{k_t}{D_3}\left[\dfrac{D_4}{D_6}\dfrac{\sin\alpha}{\alpha} - \left(1 - \dfrac{D_4 k_t\cos\alpha}{D_3 D_6}\right)\dfrac{\sin\alpha - \alpha\cos\alpha}{\alpha}\right] \\ K = \dfrac{\rho q - N_{thrust}D_1 D_7}{(D_1 + D_2)(D_1 D_7 - 1) - D_1 D_8} \end{cases} \tag{23}$$

By substituting those coefficients into Eq. (17), the maximum compressive stress at the crown point of the arch can be written as a function of the external pressure. Since the plastic collapse is defined by material yielding, therefore, the buckling pressure P_{arch} of the arch in the post-contact phase can be worked out as

$$\frac{N_{cr}}{t_c} + \frac{6M_{cr}}{t_c^2} = \sigma_y - \sigma_{con} \tag{24}$$

By substituting Eqs. (9) and (17) into Eq. (24), the buckling pressure P_{arch} can be calculated. Finally, the plastic critical pressure $P_{y,cr}$ of the flexible risers with initial imperfections is obtained by

$$P_{y,cr} = P_{con} + P_{arch} \tag{25}$$

3.3. Separation point at the moment of collapse

If the position, i.e. R_s and β_{cr}, of the separation point at the moment of collapse is determined, the arch geometry can also be determined with Eq. (10) or (11), followed by the calculation of the critical pressure with the above-mentioned approach. However, the position of the point where the carcass separates from the pressure armor is not easy to be determined since it is affected by initial ovalization and gap, and the bending stiffness ratio between the outer and the inner layers as well.

In order to tackle this problem, a formula is needed to estimate the R_s at the collapse moment. Since this separation point always lies on the inner surface of the pressure armor, then the value of R_s is mainly decided by the internal radius of the pressure armor, influenced by the stiffness of the armor wall. Considering two extreme conditions: (1) the surrounded pressure armor is rigidity; (2) the stiffness of the pressure armor is close to zero, or the inner surface of the pressure armor is too far away from the liner to provide supports before the collapse of the carcass. The actual value of R_s is bounded by the two extreme values from these two conditions, which should have $R_{p.i} < R_s < R_{c,H'}$, as shown in Fig. 10. Where $R_{p.i}$ is the internal radius of the pressure armor in condition (1) while

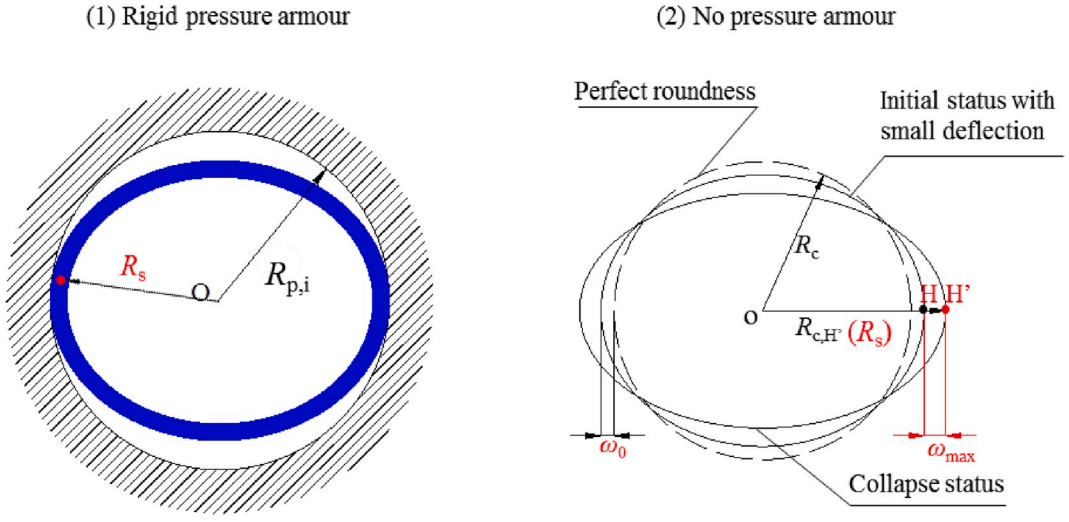

Fig. 10. Two extreme conditions regarding the stiffness of the pressure armor.

$R_{c,H'}$ is the semi-major axis of the elliptical carcass at the collapse moment in condition (2).

After taking the factors such as initial deflection ω_0 and gap ω_g, wall thickness reduction of the liner t_{lr} into account, such a formula is proposed

$$R_s = R_c + \omega_0 + \omega_g + t_{lr} + (\omega_{max} - \omega_g - t_{lr})\left(\frac{\omega_0 + \omega_g + t_{lr}}{\omega_{max} + \omega_0}\right)^{\varphi_k}, 0 \le \omega_g + t_{lr} < \omega_{max} \tag{26}$$

with the value of R_s that estimated from Eq. (26), the buckling pressure P_{arch} can be determined by decreasing β_{cr} (from $\pi/2$ to 0) continually until the bending moments of the attached and detached portions at the separation point equal to each other, as shown in Fig. 11. The bending moment for the detached arch ends can be calculated by Eq. (17). For the attached portion, the bending moment at the separation point is obtained by Ref. [20].

$$M_1 = E_c I_c\left(\frac{1}{\rho_{cr}} - \frac{1}{R_s}\right) \tag{27}$$

Once M and M_1 are equal, the angle β_{cr} can be determined as well as the buckling pressure P_{arch} of the arch. A flowchart that shows the whole procedure is given as Fig. 12.

4. Verification of the proposed analytical model

The above sections clarify the development of the proposed analytical model for predicting the wet collapse pressure of flexible pipes with initial ovalization and gap. To verify its reliability, numerical simulation is employed as a tool to examine the reliability of this developed model on collapse prediction. The case study is explained in section 4.1 while in section 4.2, discussion is given based on the results from the studied case.

4.1. Case description

For verification purposes, a 2D FE equivalent ring model with variable initial ovalization and gap was constructed, as shown in Fig. 13. Half of the cross section with symmetric boundary conditions was built with Abaqus 6.13. With this half cross-section 2D model, the initial ovalization could be introduced onto the carcass in either singly or doubly way for triggering the corresponding bi-symmetrical or symmetrical collapse shape.

This 2D FE model was developed from a prototype model that presented by Gay Neto and Martins [8], which is a 3D FE model of a 4" flexible pipe with three layers, i.e., the carcass, the inner liner and the pressure armor. In the prototype model, the carcass was built with a detailed profile while the liner and pressure armor were represented as two homogeneous equivalent layers, as shown in Fig. 14. With the material properties presented in their previous work [29], the equivalent layer method could be employed to determine the equivalent properties of the carcass for this 2D FE model. The reliability of the 2D FE model on predicting the collapse pressure was examined before using it for the verification of the analytical model.

Table 1 lists the geometric and material data of the prototype model [8,29]. Geometric details of the carcass profile are given in the source references. The material stress-strain curves of the liner are shown in Fig. 15. With those data, a strain energy-based equivalent layer method was employed to determine the equivalent properties of the carcass. This strain energy-based equivalent layer is

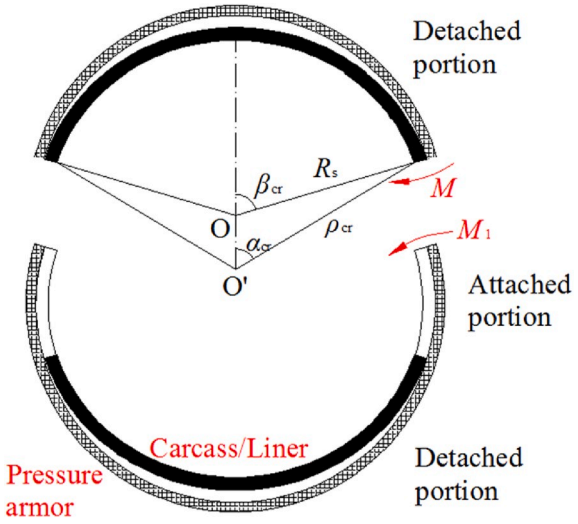

Fig. 11. Bending moments at the separation point.

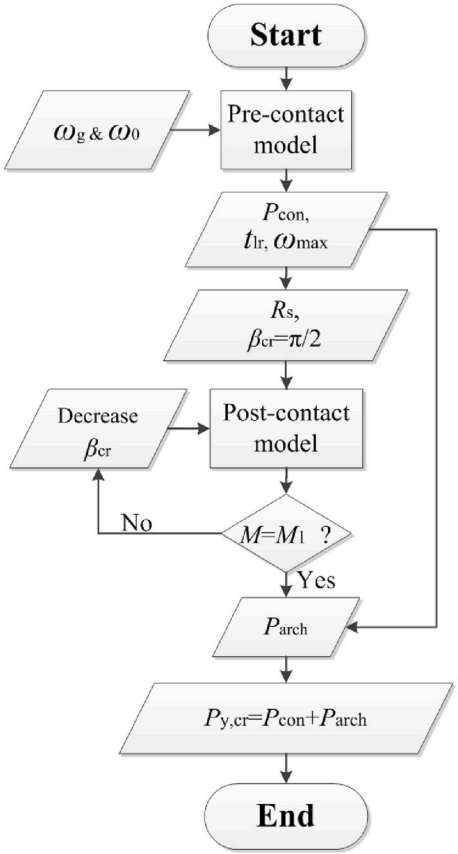

Fig. 12. Flowchart of the whole analytical scheme.

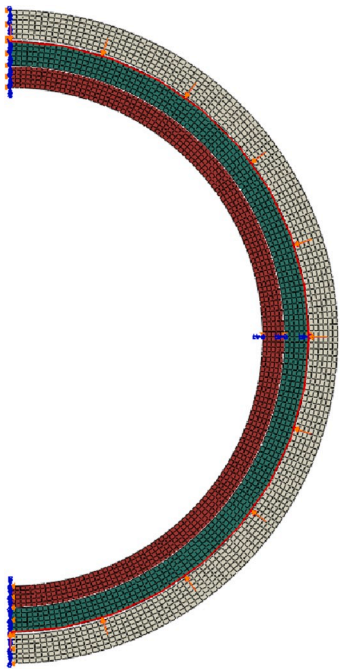

Fig. 13. 2D FE ring model for verification.

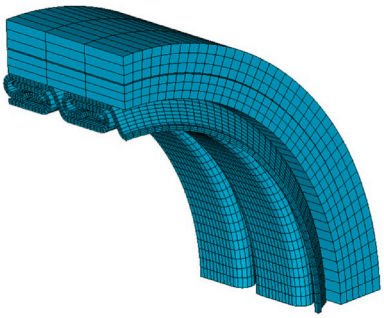

Fig. 14. 3D FE model of a 4″ flexible pipe [8].

Table 1
Geometric and material properties [8,29].

Model	Carcass	Liner	Pressure armor
Internal diameter (mm)	101.6	114.4	var.
Layer thickness (mm)	6.40	5.00	5.86
Young's Modulus (GPa)	200	–	207
Poisson's Ratio	0.3	0.45	0.3
Tangent Modulus (GPa)	2.02	–	50.00
Yield stress (MPa)	600	–	650

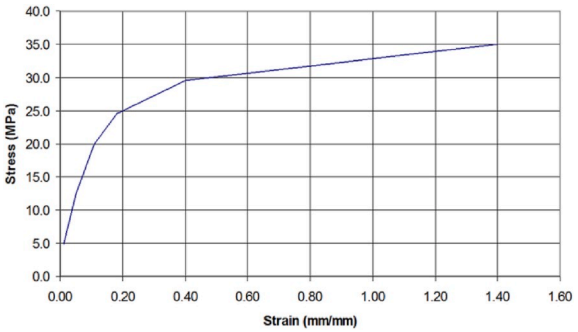

Fig. 15. Stress-strain curve of the liner [29].

proposed in our previous research [30], based on two equivalences between structures, i.e. strain energy, and membrane stiffness. The equivalent thickness, Young's Modulus and yield stress for ring models are 4.5 mm, 158 GPa and 473 GPa, respectively. Those equivalent properties along with other layer data were used to construct the 2D FE ring model.

The reliability of this 2D FE model for critical pressure prediction were examined by the 3D FE model that given by Gay Neto [8]. That 3D FE model gave a critical pressure of 24.90 MPa for the case "B1", which only considered a 0.5% initial ovalization on its carcass. The critical pressure predicted by the equivalent 2D FE model was 23.43 MPa, with a 5.9% difference from the result in Ref. [8]. It should be noted that the collapse in 2D FEA is a plane-stress issue while the 3D FE model studied the collapse in a plane-strain state. For a better comparison, the above result was transferred to 25.75 MPa to consider a plane-strain state by including Poisson's ratio. Therefore, the errors was further reduced to −3.4%. It indicated that the 2D FE model is trustworthy for the following verification.

Parametric studies were done to examine the reliability of the analytical approach for different level of initial ovalization and interlayer gap. Firstly, three levels of initial ovalization were considered as 0.5%, 1.0%, and 2.0%. The ovality were imposed to the carcass and the liner in either singly or doubly type in order to trigger corresponding "heart" or "eight" modes. The surrounded pressure armor remains a perfectly circular cross section. Secondly, an initial gap was introduced between the pressure armor and the liner while the initial ovalization of the carcass and the liner was fixed to 0.5%. According to the numerical analysis, the ultimate gap width for the carcass collapses with layer contacts is 0.36 mm; therefore, the gap width considered in the cases has a range that varies from 0 to 0.3 mm. The calculated wet collapse pressure of the 4″ flexible pipe with initial imperfections were collected and listed with tables in Section 4.2.

4.2. Results and discussion

The predictions given by the proposed analytical model were compared against the corresponding numerical results. Table 2 shows the critical pressure that calculated analytically or numerically for varied singly/doubly initial ovalization. The wet collapse pressure predicted by the analytical model correlates quite well with the numerical results, with a difference below 10%. From the results, it can be seen that the confined carcass collapses with a bi-symmetrical shape yields a higher critical pressure than the one with symmetrical shape. This phenomenon is probably caused by the definition of initial ovalization that given by API 17B [26], which imposes a larger initial deflection on the singly ovalized carcass for the same level of initial ovalization.

In addition, the numerical simulation shows a one-side ovalization could also trigger the detachment on the other side of the carcass, as displayed in Fig. 16. For a carcass with initial ovalization, there is a length shortage in its circumference comparing with the one in a perfect roundness. In the numerical simulation of the singly ovalized pipe, the length shortage is spread over two detached portions rather than one. As a result, the carcass in numerical simulation has a smaller degree of ovalization than that in analytical models and hence performs a higher critical pressure. This explains why the analytical model gives much lower prediction for the singly ovality cases, since it assumes the singly ovalized carcass always collapses with a symmetrical shape.

It should be noted that a singly initial ovalization would still lead to a "heart mode", regardless of whether "symmetrical" or "bi-symmetrical" shape develops. This is because the snap-through can only occur at a single point if the cross section is not in a perfect symmetric shape. Once the snap-through takes place, the release of strain energy will stabilize any other possible failure points of the carcass immediately. This may explain why the "heart" mode is a typical mode shape that usually found in wet collapse tests [16].

The comparison of critical pressure regarding initial gap is given in Table 3. According to the results listed in Table 3, the proposed analytical model provides conservative estimation of the collapse pressure with comparison to numerical results. Notable differences occur between the numerical and analytical predictions, especially for the large gap cases. This is because the proposed analytical model treats the pressure armor as springs which could only provide the constraints on the radial deformation of the carcass from their contact regions. In the numerical simulation, however, the surrounded pressure armor restrains not only the radial deformation but also the rotation of the detached portions of the carcass. Therefore, the bending stiffness of the carcass was largely enhanced after getting in contact with the pressure armor.

For the flexible pipes, its wet collapse pressure is mainly decided by the bending and membrane stiffness of the carcass [28,31]. When the encased carcass is deformed from a perfect roundness to an ovalized shape under the external pressure, the dominated stiffness of the carcass for collapse resistance is gradually switched from the hoop membrane stiffness to the bending stiffness. With the increase of the initial gap width, the carcass is more oval-shaped when the contact occurs. Therefore, the bending stiffness of the carcass plays an important role in those large gap cases. Since the analytical model neglects the rotation restraints from the pressure armor, it underestimates the bending stiffness of the carcass in the post-contact phase. As a result, much conservative predictions are given by the analytical solution.

5. Conclusions

With more and more ultra-deep water reservoirs are being targeted for oil and gas production, the collapse resistance of flexible risers becomes one of the main concerns for designers. Collapse analyses are required to take initial imperfections into account since the collapse capacity is susceptible to them. This paper presents an analytical approach to predict the wet collapse pressure for the flexible risers with initial ovality and gap. Stability theories of ring and arched structures are employed to address the collapse behaviors of the encased carcass subjected to wet collapse. With those theories, the plastic wet collapse pressure of the imperfect flexible pipes can be determined.

Numerical simulation was adopted as a tool in the case studies to verify this proposed analytical model. The verification shows the analytical model has a good performance on predicting the wet collapse pressure for flexible pipes regarding the initial ovalization. The prediction given by the analytical model is in good agreement with the numerical results, with differences that no more than 10%. By contrast, the performance of the analytical approach was not as good as that in ovality cases. The collapse strength of the carcass in the analytical model was underestimated due to the neglect of rotation restraint imposed by pressure armor. As a result, the analytical approach gives much conservative prediction on wet collapse pressure for the flexible risers with initial gaps.

Additionally, one noticeable phenomenon from the case study is the comparison differences displayed in the singly ovality cases are relatively larger than those in doubly ones. To trigger different collapse modes of the carcass, the initial ovalization was imposed as singly and doubly type respectively in all the cases. For the analytical model, it assumes the singly ovalized carcass always collapses

Table 2
Comparison of collapse pressure between FE and analytical models for singly and doubly ovality.

Initial ovalization	Critical pressure (MPa)					
	singly			doubly		
	FEA	Analyt.	Diff. (%)	FEA	Analyt.	Diff. (%)
0.5%	22.68	20.48	9.72	23.43	23.21	0.94
1.0%	20.63	18.73	9.19	21.97	21.95	0.11
2.0%	17.60	17.39	1.17	19.71	20.42	−3.63

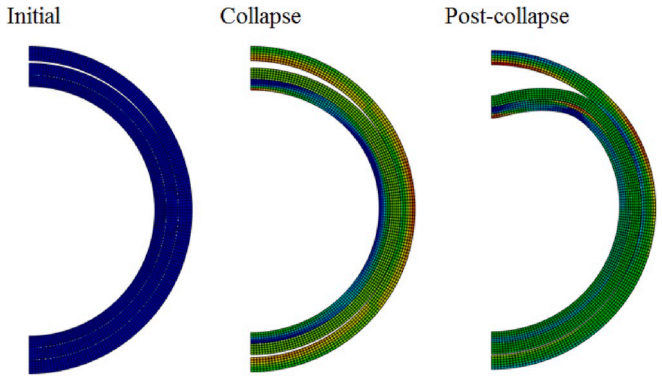

Fig. 16. Collapse process of the singly ovalized pipe performed by 2D FE model.

Table 3
Comparison of collapse pressure between FE and analytical models for interlayer gap.

Initial gap (mm)	Critical pressure (MPa)					
	singly ovality			doubly ovality		
	FEA	Analyt.	Diff. (%)	FEA	Analyt.	Diff. (%)
0.05	22.41	19.44	13.27	23.09	20.40	11.64
0.1	22.14	18.33	17.18	22.83	18.92	17.10
0.2	21.61	15.38	28.82	22.26	16.83	24.39
0.3	21.11	14.12	33.13	21.72	16.68	23.21

with an "symmetrical" shape. However, the simulation shows that a singly initial ovalization could also trigger a approximate "bi-symmetrical shape" of the carcass when coming to collapse. This results in a smaller maximum ovalization level of the carcass and hence increases the collapse pressure of the FE models.

Up to now, analytical models that developed for collapse prediction of flexible pipes are limited, especially for the initial imperfections. Collapse pressure of an actual flexible pipe is not easy to be predicted since it is affected by those imperfections. In this regard, this paper presents an analytical model which can take initial ovalization and interlayer gap into account, aiming to facilitate the collapse analysis of flexible risers in its design stage. The verification given by numerical simulation indicates that this analytical model can be a good choice for ovalization issue. As for interlayer gap, this model should be further improved to enhance its prediction accuracy.

Acknowledgments

This work was supported by the China Scholarship Council [grant number 201606950011].

References

[1] Shen Y, Jukes P. Technical challenges of unbonded flexible risers in HPHT and deepwater operations. In: Proceedings of the 25th international ocean and polar engineering conference. Hawaii, USA: International Society of Offshore and Polar Engineers (ISOPE), Kona, Big Island; 2015.
[2] Brouard Y, Seguin B, Germanetto F. Riser solutions for turret moored FPSO in Arctic conditions. In: Proc. 2016 offshore tech conf, St. John's, Newfoundland and Labrador, Canada; 2016. Paper No. OTC-27389-MS.
[3] National Oilwell Varco. Floating production systems: dynamic flexible risers. NOV; 2014.
[4] Lohr C, Pena M. Stones development: a pioneering management philosophy for enhancing project performance and safety. In: Proc. 2017 offshore tech conf, Houston, USA; 2017. Paper No. OTC-27674-MS.
[5] Bectarte F, Secher P, Felix-Henry A. Qualification testing of flexible pipes for 3,000m water depths. In: Proc. 2017 offshore tech conf, Houston, USA; 2011. Paper No. OTC-21490-MS.
[6] Silva JV, Damiens A. 3,000m water depth flexible pipe configuration portfolio. In: Proc. 2016 offshore tech conf, Houston, USA; 2016. Paper No. OTC-26933-MS.
[7] Crome T. Experiences from design and operation, learning and improvements. Technip; 2013.
[8] Gay Neto A, Martins CA. Flexible pipes: influence of the pressure armor in the wet collapse resistance. J Offshore Mech Arctic Eng 2014;136(3):031401.
[9] Bai Y, Yuan S, Cheng P, Han P, Ruan W, Tang G. Confined collapse of unbonded multi-layer pipe subjected to external pressure. Compos Struct 2016;158:1–10.
[10] Cooke N, Kenny S. Comparative study on the collapse response of flexible pipe using finite element methods. In: Proceedings of the 33rd international conference on ocean, offshore and arctic engineering. San Francisco, California, USA: American Society of Mechanical Engineers; 2014. OMAE2014-23306.
[11] Axelsson G, Skjerve H. Flexible riser carcass collapse analyses-sensitivity on radial gaps and bending. In: Proceedings of the 33rd international conference on ocean, offshore and arctic engineering. San Francisco, California, USA: American Society of Mechanical Engineers; 2014. OMAE2014-23922.
[12] Davidson M, Fernando US, Donnell B, Bell A, Ramsay A. Prediction of extruded profile shape of polymer barrier in flexible pipes. In: Proceedings of the 26th international ocean and polar engineering conference. Rhodes,Greece: International Society of Offshore and Polar Engineers (ISOPE); 2016.

[13] Sousa JRM, Protasio MK, Sagrilo LVS. Equivalent layer approaches to predict the bisymmetric hydrostatic collapse strength of flexible pipes. In: Proceedings of the 37th international conference on ocean, offshore and arctic engineering. Madrid, Spain: American Society of Mechanical Engineers; 2018. OMAE2018-78146.
[14] Zhang Y, Chen B, Qiu L, Hill T, Case M. State of the art analytical tools improve optimization of unbonded flexible pipes for deepwater environments. In: Proc. 2003 offshore tech conf, Houston, USA; 2003. Paper No. OTC-15169.
[15] Malta ER, Martins CA, Gay Neto A, Toni FG. An investigation about the shape of the collapse mode of flexible pipes. In: Proceedings of the 22nd international ocean and polar engineering conference. Rhodes,Greece: International Society of Offshore and Polar Engineers (ISOPE); 2012.
[16] Paumier L, Averbuch D, Felix-Henry L. Flexible pipe curved collapse resistance calculation. In: Proceedings of the 28th international conference on ocean, offshore and arctic engineering. Honolulu, Hawaii, USA: American Society of Mechanical Engineers; 2009. OMAE2009-79117.
[17] Lu J, Ma F, Tan Z, Sheldrake T. Bent collapse of an unbonded rough bore flexible pipe. In: Proceedings of the 27th international conference on ocean, offshore and arctic engineering. Estoril, Portugal: American Society of Mechanical Engineers; 2008. OMAE2008-57063.
[18] Gay Neto A, Martins CA, Malta ER, Tanaka RL, Godinho CAF. Simplified finite element models to study the wet collapse of straight and curved flexible pipes. J Offshore Mech Arctic Eng 2017;139(6):061701.
[19] https://doi.org/10.1115/OMAE2019-95642. [Accessed 11 November 2019].
[20] Timoshenko SP, Gere J. Theory of elastic stability. New York, USA: McGraw-Hill; 1963.
[21] Fergestad D, Løtveit SA. Handbook on design and operation of flexible pipes. MARINTEK: Technical Report; 2017.
[22] Glock D. Überkritisches verhalten eines starr ummantelten kreisrohres bei wasserdruck von außen und temperaturdehnung (Post-critical behavior of a rigidly encased circular pipe subjected to external water pressure and thermal extension). Der Stahlbau 1977;46:212–7.
[23] Boot JC. Elastic buckling of cylindrical pipe linings with small imperfections subject to external pressure. Trenchless Technol Res 1998;12(1–2):3–15.
[24] Thépot O. Structural design of oval-shaped sewer linings. Thin-Walled Struct 2001;39:499–518.
[25] Chen YG, Liu J, Zhu LF, Tan ZM, Karabelas G. An analytical approach for assessing the collapse strength of an unbonded flexible pipe. J Mar Sci Appl 2015;14:196–201.
[26] API. Recommended practice for flexible pipe API RP 17B. fifth ed. Washington: American Petroleum Institute; 2014.
[27] Lo KH, Zhang JQ. Collapse resistance modeling of encased pipes. In: Eckstein Dave, editor. Buried plastic pipe technology: 2nd volume. ASTM STP 1222. Philadelphia: American Society for Testing and Materials; 1994.
[28] Tong G. In-plane stability of steel structures. Beijing: China Architecture & Building Press; 2005.
[29] Gay Neto A, Martins CA. A comparative wet collapse buckling study for the carcass layer of flexible pipes. J Offshore Mech Arctic Eng 2012;134(3):031701.
[30] Li X, Jiang X, Hopman H. A strain energy-based equivalent layer method for the prediction of critical collapse pressure of the flexible risers. Ocean Eng 2018;164:248–55.
[31] Karnovsky IA. Theory of arched structures: strength, stability, vibration. Springer Science & Business Media; 2011.